J Membrane Biol (2012) 245:531–543
DOI 10.1007/s00232-012-9434-6

# Molecular Dynamics Simulations of Lipid Membrane Electroporation

**Lucie Delemotte · Mounir Tarek**

Received: 22 December 2011 / Accepted: 30 April 2012 / Published online: 30 May 2012


**Abstract** The permeability of cell membranes can be transiently increased following the application of external electric fields. Theoretical approaches such as molecular modeling provide a significant insight into the processes affecting, at the molecular level, the integrity of lipid cell membranes when these are subject to voltage gradients under similar conditions as those used in experiments. This article reports on the progress made so far using such simulations to model membrane—lipid bilayer—electroporation. We first describe the methods devised to perform in silico experiments of membranes subject to nanosecond, megavolt-per-meter pulsed electric fields and of membranes subject to charge imbalance, mimicking therefore the application of low-voltage, long-duration pulses. We show then that, at the molecular level, the two types of pulses produce similar effects: provided the TM voltage these pulses create are higher than a certain threshold, hydrophilic pores stabilized by the membrane lipid headgroups form within the nanosecond time scale across the lipid core. Similarly, when the pulses are switched off, the pores collapse (close) within similar time scales. It is shown that for similar TM voltages applied, both methods induce similar electric field distributions within the membrane core. The cascade of events following the application of the pulses, and taking place at the membrane, is a direct consequence of such an electric field distribution.

**Keywords** Millisecond pulse · Nanopulse · Electric field · Nanopore

L. Delemotte · M. Tarek
UMR Structure et Réactivité des Systèmes Moléculaires Complexes, CNRS-Université de Lorraine, Vandoeuvre-lès-Nancy, Cedex, France

*Present Address:*
L. Delemotte
Institute for Computational Molecular Science, Temple University, Philadelphia, PA 19122, USA

M. Tarek (✉)
Unité Mixte de Recherches CNRS UHP 7565, Université de Lorraine, Campus Science Grignard BP 239, 54506 Vandoeuvre-lès-Nancy, Cedex, France
e-mail: mounir.tarek@univ-lorraine.fr

## Introduction

Electroporation disturbs transiently or permanently the integrity of cell membranes (Eberhard et al. 1989; Nickoloff 1995; Li 2008). These membranes consist of an assembly of lipids, proteins and carbohydrates that self-organize into a thin barrier that separates the interior of cell compartments from the outside environment (Gennis 1989). The main lipid constituents of natural membranes are phospholipids that arrange themselves into a two-layered sheet (a bilayer). Experimental evidence suggests that the effect of an applied external electric field to cells is to produce aqueous pores specifically in the lipid bilayer (Abidor et al. 1979; Benz et al. 1979; Weaver and Chizmadzhev 1996; Weaver 2003; Chen et al. 2006). Information about the sequence of events describing the electroporation phenomenon can therefore be gathered from measurements of electrical currents through planar lipid bilayers along with characterization of molecular transport of molecules into (or out of) cells subjected to electric field pulses. It may be summarized as follows: the application of electrical pulses induces rearrangements of the membrane components (water and lipids) that ultimately lead to the formation of aqueous hydrophilic pores (Abidor et al. 1979; Benz et al. 1979; Weaver and Chizmadzhev 1996; Weaver 2003; Chen et al. 2006; Pucihar et al. 2006),

whose presence increases substantially the ionic and molecular transport through the otherwise impermeable membranes (Pucihar et al. 2008).

The key features of electroporation are based on theories involving stochastic pore formation (Chen et al. 2006). In erythrocyte membranes, large pores could be observed using electron microscopy (Chang 1992); but in general, direct observation of the formation of nano-sized pores is not possible with conventional techniques. Furthermore, due to the complexity and heterogeneity of cell membranes, it is difficult to describe and characterize their electroporation in terms of atomically resolved processes. Atomistic simulations in general, and molecular dynamics (MD) simulations in particular, have proven to be effective for providing insights into both the structure and the dynamics of model lipid membrane systems in general (Tieleman et al. 1997; Tobias et al. 1997; Forrest and Sansom 2000; Feller 2000, 2008; Tobias 2001; Mashl et al. 2001; Saiz and Klein 2002a; Anézo et al. 2003; Berkowitz et al. 2006; Lindahl and Sansom 2008; Edholm 2008; Marrink et al. 2009).

Recent studies have shown that the method is suitable for investigating electroporation phenomena. Several MD simulations have recently been conducted in order to model the effect of electric field on membranes (Hu et al. 2005; Tieleman 2004; Tarek 2005; Bockmann et al. 2008; Ziegler and Vernier 2008), providing perhaps the most complete molecular model of the electroporation process of lipid bilayers. This article reviews the progress made so far using such atomistic simulations to model lipid bilayer electroporation.

The effects of an electric field on a cell may be described considering the latter as a dielectric layer (cell surface membrane) embedded in conductive media (internal, cytoplasm; external, extracellular media). When relatively low-field pulses of microsecond or millisecond duration are applied to this cell (by placing, for instance, the cell between two electrodes and applying a constant voltage pulse), the resulting current causes accumulation of electrical charges at both sides of the cell membrane. The time required to charge the surface membrane is dependent upon the electrical parameters of the medium in which it is suspended. For a spherical cell it is estimated using equivalent network RC circuits in the 100-ns time scale (Hu et al. 2005; Beebe and Schoenbach 2005; Vasilkoski et al. 2006; Sundararajan 2009; Deng et al. 2003). A charging time constant in the range of hundreds of nanoseconds was also obtained from derivations based on the Laplace equation (see, e.g., Pauly and Schwan 1959 for the first-order analysis on a spherical vesicle; Kotnik et al. 1998 for the second-order analysis; and Kotnik and Miklavcic 2006 for the second-order analysis for two concentric spherical vesicles, i.e., modeling an organelle).

If, on the other hand, the pulse duration is short enough relative to the charging time constant of the resistive-capacitive network formed by the conductive intracellular and extracellular fluids and the cell membrane dielectric, which is the case for nanosecond pulses, the electric field acts directly and mainly on the cell membrane.

Simulations allow one to perform in silico experiments under both conditions, i.e., submitting the system either to nanosecond, megavolt-per-meter pulsed electric fields or to charge imbalance, mimicking therefore the application of low-voltage, long-duration pulses. Here, we describe the results of such simulations, after a brief general introduction to MD simulations of membranes.

## Materials and Methods

### MD Simulations

The MD simulation presented here was carried out using the program NAMD targeted for massively parallel architectures (Kalé et al. 1999; Bhandarkar et al. 2002). The systems were examined in the NPT (1 atm and 300 K) or NVT (300 K) ensembles employing Langevin dynamics and the Langevin piston method. The equations of motion were integrated using the multiple time-step algorithm. A time step of 2.0 fs was employed. Short- and long-range forces were calculated every two and four time steps, respectively. Chemical bonds between hydrogen and heavy atoms were constrained to their equilibrium value. Long-range, electrostatic forces were taken into account using a fast implementation of the particle mesh Ewald (PME) approach (Darden et al. 1993; Essmann et al. 1995), with a direct space sum tolerance of $10^{-6}$ and a spherical truncation of 11 Å.

Bond stretching, valence angle deformation, torsional and nonbonded parameters and nonbonded interaction were all extracted from the all-atom CHARMM force field (MacKerell et al. 1998). For the lipid palmitoyl-oleyl-phosphatidylcholine (POPC) we used the united atom representation for the acyl chains.

### Electrostatic Properties

The electrostatic potential, $\phi(z)$, along the lipid bilayer normal, $z$, was derived from MD simulations using Poisson's equation and expressed as the double integral of $\rho(z)$, the molecular charge density distributions:

$$\phi(z) = \phi(z) - \phi_0 = \frac{-1}{\varepsilon_0} \int_0^Z \int \rho(z'') \mathrm{d}z'' \mathrm{d}z' \qquad (1)$$

As a reference, $\phi_0$ is set to zero in the upper bulk. Finally, the transmembrane (TM) voltage was calculated as the difference between the electrostatic potentials measured at the upper and lower baths.

The electric field profiles deriving from the charge distribution, called here "local electric fields," were obtained from the electrostatic profiles using $\partial\phi(z)/\partial z$.

Three-dimensional (3D) maps of the electrostatic potential characterizing the systems were generated by solving numerically the Poisson equation. This calculation was performed employing the PMEPot module of the visualization program VMD (Humphrey et al. 1996). Instantaneous values of the electrostatic potential were averaged over 100-ps segments. The first derivative of the electrostatic potential was evaluated using OpenDX (http://www.opendx.org), an open–source visualization software package, to yield the 3D maps of the electric field. The electric properties of the bilayers described in this contribution were visualized with OpenDX and the CMSP Chemistry module (Gillilan and Wood 1995).

## Modeling Membrane Electroporation

"Molecular dynamics" refers to a family of computational methods aimed at simulating macroscopic behavior through the numerical integration of the classical equations of motion of a microscopic, many-body system. Macroscopic properties are expressed as functions of particle coordinates and/or momenta, which are computed along a phase space trajectory generated by classical dynamics (Allen and Tildesley 1987; Leach 2001) When performed under conditions corresponding to laboratory scenarios, MD simulations can provide a detailed view of the structure and dynamics of a macromolecular system. They can also be used to perform "computer experiments" that cannot be carried out in the laboratory, either because they do not represent a physical behavior or because the necessary controls cannot be achieved. Simulations are usually performed on a small number of molecules (few tens to few hundred thousand atoms), the system size being limited, of course, by the speed of execution of the programs and the availability of computer power. In order to eliminate edge effects and to mimic a macroscopic system, simulations of condensed phase systems consider a small patch of molecules confined in a central simulation cell and replicate the latter using periodic boundary conditions (PBCs) in the three directions of Cartesian space. For membranes, for instance, the simulated system would correspond to a small fragment of either a black film, a liposome or multilamellar oriented lipid stacks deposited on a substrate (Lindahl and Edholm 2000; Marrink and Mark 2001).

Traditionally, phospholipids have served as models for investigating in silico the structural and dynamic properties of membranes. From both a theoretical and an experimental perspective, zwitterionic phosphatidylcholine (PC) lipid bilayers constitute the best-characterized systems (Chiu et al. 1999; Rög et al. 2002; Saiz and Klein 2001; Feller et al. 2002) (Fig. 1). More recent studies have considered a variety of alternative lipids, featuring different, possibly charged, headgroups (Berkowitz and Raghavan 1991; Damodaran and Merz 1994; Cascales et al. 1996; Mukhopadhyay et al. 2004; Chiu et al. 2003) and more recently mixed bilayer compositions (Pandit et al. 2003; Patel and Balaji 2008; Dahlberg and Maliniak 2008; Gurtovenko and Vattulainen 2008; Vacha et al. 2009; Rog et al. 2009; Li et al. 2009). Despite their simplicity, bilayers built from PC lipids represent remarkable test systems to probe the computation methodology and to gain additional insight into the physical properties of

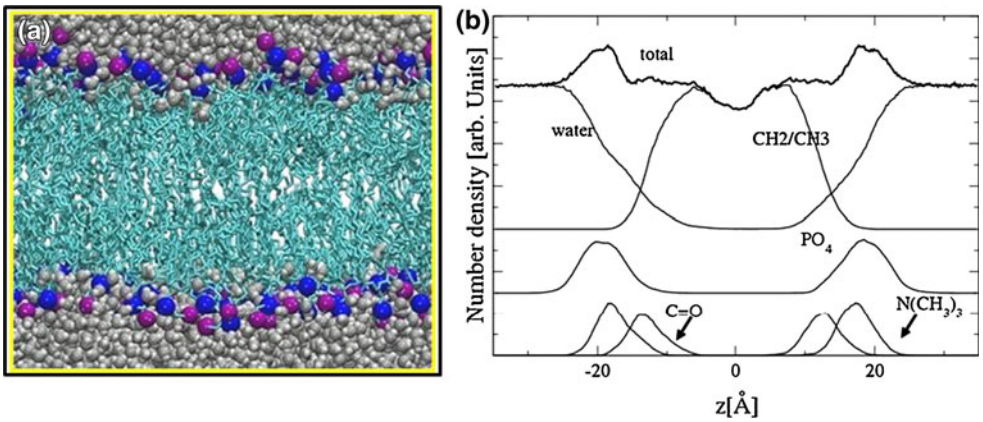


**Fig. 1** **a** Configuration of a palmitoyl-oleyl-phosphatidylcholine (POPC)-hydrated bilayer system from a well-equilibrated, constant-pressure MD simulation performed at 300 K. Only the molecules in the simulation cell are shown. Water molecules (O, *gray*; H, *white*) and the phosphate (*blue*) and nitrogen (*purple*) atoms of the lipid headgroups are depicted by their van der Waals radii, and the acyl chains (*cyan*) are represented as sticks. **b** Number density profiles (arbitrary units) along the bilayer normal, $z$, averaged over 2 ns of the MD trajectory. The total density, water and hydrocarbon chain contributions are indicated, along with those from the POPC headgroup moieties. The bilayer center is located at $z = 0$ (Color figure online)

membranes (Tobias et al. 1997; Tobias 2001; Anézo et al. 2003; Chipot et al. 2005).

Up to recently, most membrane models consisted of simulating fully hydrated, pure phospholipid bilayers, without taking into account the effect of salt concentration (see sections below). For such systems, the average structure of the lipid–water interface at the atomic scale may be provided by the density distributions of different atom types along the bilayer normal (Fig. 1), which can be measured experimentally on multilamellar stacks by neutron and X-ray diffraction techniques (Wiener and White 1992) as well as calculated from MD simulations. These distributions highlight the composition and properties of the membrane that appears as a broad hydrophilic interface, with only a thin slab of pure hydrocarbon fluid in the middle (Fig. 1). They indicate clearly the roughness of the lipid headgroup area and how water density decays smoothly from the bulk value and penetrates deeply into the bilayer at a region delimiting the membrane–water interface.

## Electroporation Induced by Direct Effect of an Electric Field

In the following we describe the methods/protocols and results obtained from modeling the effect of a direct electric field on lipid membranes. In simulations, it is possible to apply "directly" a constant electric field, $\vec{E}$, perpendicular to the membrane (lipid bilayer) plane. In practice, this is done by adding a force, $\vec{F} = q_i\vec{E}$, to all the atoms bearing a charge, $q_i$ (Zhong et al. 1998; Yang et al. 2002; Tieleman et al. 2001; Crozier et al. 2001; Roux 2008). MD simulations adopting such an approach have been used to study membrane electroporation (Hu et al. 2005; Tieleman 2004; Tarek 2005; Bockmann et al. 2008; Ziegler and Vernier 2008) and lipid externalization (Vernier et al. 2006a), to activate voltage-gated $K^+$ channels (Treptow et al. 2004) and to determine the transport properties of ion channels (Aksimentiev and Schulten 2005; Khalili-Araghi et al. 2006; Sotomayor et al. 2007; Chimerel et al. 2008). Quite noticeably, these protocols were initially applied in simulations of membranes to study classical electroporation. It was only later that it became possible experimentally to use nanosecond pulses. It turns out that such protocols model rather the effects of nanosecond, megavolt-per-meter pulsed electric fields that are too short to charge the membrane capacitor. For practical reasons and in order to avoid charge (ions) accumulations when the field is applied, it is recommended that this method be used when modeling lipid bilayers in the absence of salts. Indeed, in contrast to experiments, because of the small size of the systems ($\sim$10 nm in the $\vec{E}$ field direction), even nanosecond pulses can induce "notable" charge reorganization.

The consequence resulting from high electric field application to the system stems from the properties of the membrane and from the simulations setup conditions: pure lipid membranes exhibit a heterogeneous atomic distribution across the bilayer, to which are associated charges and molecular dipole distributions. Phospholipid headgroups adopt in general a preferential orientation. For hydrated PC bilayers at temperatures above the gel to liquid crystal transition, the PC dipoles point on average 30° away from the membrane normal (Tobias 2001; Saiz and Klein 2002b). The organization of the phosphate ($PO_4^-$), choline ($N[CH_3]_3^+$) and carbonyl (C=O) groups of the lipid headgroup hence give rise to a permanent dipole, and the solvent (water) molecules bound to the lipid headgroup moieties tend to orient their dipoles to compensate the latter (Gawrisch et al. 1992). The electrostatic characteristics of the bilayer may be gathered from estimates of the electrostatic profile, $\phi(z)$, that stems from the distribution of all the charges in the system.

For lipid bilayers, most of which are modeled without consideration of a salt concentration, an applied electric field acts specifically and primarily on the interfacial water dipoles (small polarization of bulk water molecules). The reorientation of the lipid headgroups appears not to be affected at very short time scales (Tarek 2005; Vernier and Ziegler 2007) and not to exceed a few degrees toward the field direction at a longer time scale (Bockmann et al. 2008). Hence, within a very short time scale, typically few picoseconds (Tarek 2005), a transverse field, $\vec{E}$, induces an overall TM potential, $\Delta V$ (Fig. 2). It is very important to note here that, because of the MD simulation setup (and the use of PBCs), $\vec{E}$ induces a voltage difference, $\Delta V \approx |\vec{E}|.L_Z$, over the whole system, where $L_z$ is the size of the simulation box in the field direction. In the example shown in Fig. 2, $L_z$ is $\sim$10 nm. The electric field (0.1 V $nm^{-1}$) applied to the POPC bilayer induces $\Delta V \sim$ 1 V.

MD simulations of pure lipid bilayers have shown that the application of electric fields of high enough magnitude leads to membrane electroporation, with a rather common poration sequence: the electric field favors quite rapidly (within a few hundred picoseconds) formation of water defects and water wires deep into the hydrophobic core (Tieleman 2004). Ultimately, water fingers forming at both sides of the membrane join up to form water channels (often termed "prepores" or "hydrophobic pores") that span the membrane. Within nanoseconds, a few lipid headgroups start to migrate from the membrane–water interface to the interior of the bilayer, stabilizing hydrophilic pores ($\sim$1–3 nm diameter) (Fig. 3). All MD studies have reported pore expansion as the electric field was

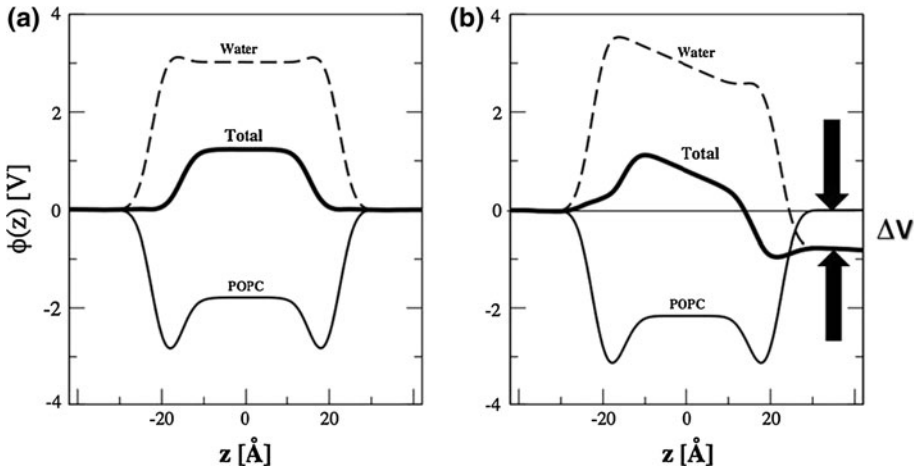


**Fig. 2** Electrostatic potential profiles, $\phi(z)$, along the membrane normal, $z$, of a POPC lipid bilayer **a** at rest and **b** subject to a transverse electric field. Shown are the contributions from water, lipid and the total electrostatic profile. Note that the TM voltage, $\Delta V$ (potential difference between the upper and lower water baths), created under electric field (**b**) is mainly due to water dipole reorientation

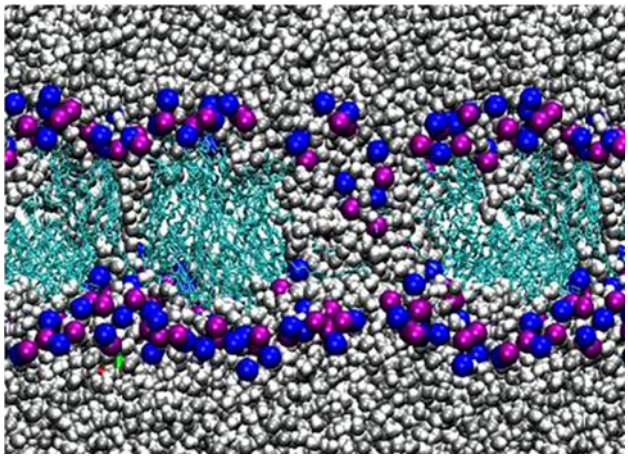

**Fig. 3** Configuration taken from an MD simulation of a large POPC bilayer, subject to an electric field generating a TM potential of $\sim$1.5 V after a 2 ns run. *Note* the simultaneous presence of water wires and of large water pores stabilized by lipid headgroups

maintained. In contrast, it was shown in one instance (Tarek 2005) that a hydrophilic pore could reseal within few nanoseconds when the applied field was switched off. Membrane complete recovery, i.e., migration of the lipid headgroups forming the hydrophilic pore toward the lipid–water interface, being a much longer process, was not observed.

For typical MD system sizes (128 lipids, 6 × 6 nm membrane cross section), most of the simulations reported a single pore formation at high field strengths. For much larger systems, multiple pore formation with diameters ranging from a few to 10 nm could be witnessed (Tieleman 2004; Tarek 2005). Such pores are in principle wide enough to transport ions and small molecules. One attempt has so far been made to investigate such a molecular transport under electroporation (Tarek 2005). In this simulation, partial transport of a 12 bp DNA strand across the membrane could be followed. The strand was considered diffused toward the interior of the bilayer when a pore was created beneath it and formed a stable DNA/lipid complex in which the lipid headgroups encapsulated the strand. The process provided support to the gene-delivery model proposed by Golzio et al. (2002), in which an "anchoring step" connecting the plasmid to permeabilized cell membranes takes place during DNA transfer assisted by electric pulses and agrees with the last findings from the same group (Paganin-Gioannia et al. 2011).

The electroporation process takes place much more rapidly under higher fields, without a major change in the pore-formation characteristics. The lowest voltages reported to electroporate a PC lipid bilayer are $\sim$2 V (Bockmann et al. 2008; Vernier and Ziegler 2007). Ziegler and Vernier (2008) reported minimum poration external field strengths for four different PC lipids with different chain lengths and composition (number of unsaturations). The authors found a direct correlation between the minimum porating fields (ranging 0.26–0.38 V nm$^{-1}$) and the membrane thickness (ranging 2.92–3.92 nm). Note that estimates of electroporation thresholds from simulations should, in general, be considered only as indicative since they are related to the time scale the pore formation may take. A field strength threshold is "assumed" to be reached when no membrane rupture is formed within the 100 ns time scale.

## Electroporation Induced by Ionic Salt Concentration Gradients

In this section, we describe the methods/protocols and results obtained from modeling the effect of a charge imbalance. Such protocols aim at mimicking the effects of low-field pulses of microsecond or millisecond duration that result in an accumulation of electrical charges at the cell membrane. Indeed, regardless of how low-intensity millisecond electrical pulses are applied, the ultimate step

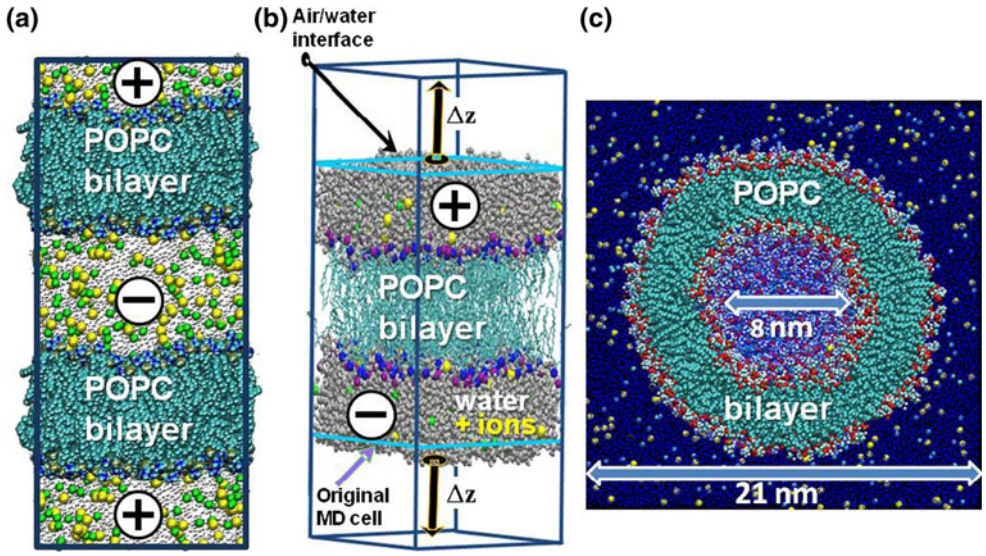


**Fig. 4** MD simulation setups of three systems using the charge imbalance method. **a** The double bilayer setup: two lipid bilayers are separated by electrolyte baths at 1 M NaCl salt concentration. Note that due to the use of PBCs (*drawn box*) the upper and lower electrolytes are in contact. $Q$ is imposed between the central water bath and the two others. **b** The single bilayer setup: here, one single bilayer is surrounded by water baths (maintained at 1 M NaCl). The original MD cell represented the classical setup and the large cell that allows for the creation of water–air interfaces. $Q$ is imposed between the lower and upper baths. **c** The liposome setup: a small, spherical liposome is embedded in a 1 M NaCl electrolyte. $Q$ is imposed between the inner and outer water baths and 3D PBCs (*drawn box*) are used

is the charging of the membrane due to ion flow. Note that here the "charging" of the membrane is not modeled. Rather, the simulations are initiated by assuming that the charging has already taken place, i.e., with a system already set at a specific (selected) charge imbalance. Evidently, in contrast to the previous protocol, here the bilayers need to be modeled at a given salt concentration. In a classical setup of membrane simulations and due to the use of 3D PBCs, the TM voltage cannot be controlled by imposing a charge imbalance across the bilayer, even when ions are present in the electrolytes. Several MD simulation protocols that can overcome this limitation have been recently devised (Fig. 4).

*The Double Bilayer Setup*

It was indeed shown that TM potential gradients can be generated by a charge imbalance across lipid bilayers by considering an MD unit cell consisting of three saltwater baths separated by two bilayers and 3D PBCs (Sachs et al. 2004) (Fig. 4a). Setting up a net charge imbalance, $Q$, between the two independent water baths at time $t = 0$ induces a TM voltage $\Delta V$ by explicit ion dynamics.

*The Single Bilayer Setup*

Delemotte et al. (2008) introduced a variant of this method where the double layer is not needed, avoiding therefore the overcost of simulating a large system. The method consists in considering a unique bilayer surrounded by electrolyte baths, each of them terminated by an air–water interface (Bostick and Berkowitz 2003). The system is set up as indicated in Fig. 4b. First, a hydrated bilayer is equilibrated at a given salt concentration using 3D PBCs. Air–water interfaces are then created on both sides of the membrane, and further equilibration is undertaken at constant volume, maintaining therefore a separation between the upper and lower electrolytes. A charge imbalance, $Q$, between the two sides of the bilayer is generated by simply displacing at time $t = 0$ an adequate number of ions from one side to the other. As far as the water slabs are thicker than 25–30 Å, the presence of air–water interfaces has no influence on the lipid bilayer properties and the membrane "feels" as if it is embedded in infinite baths whose characteristics are those of the modeled finite solutions. This method was recently successfully applied to study transport in ion channels (Delemotte et al. 2010, 2011; Treptow et al. 2009).

*Extension to Liposomes*

The availability of large computer resources has extended the realm of simulations of membrane electroporation to study systems large enough to allow modeling of small liposomes. Figure 4c represents such a liposome constructed from a POPC bilayer and equilibrated in a

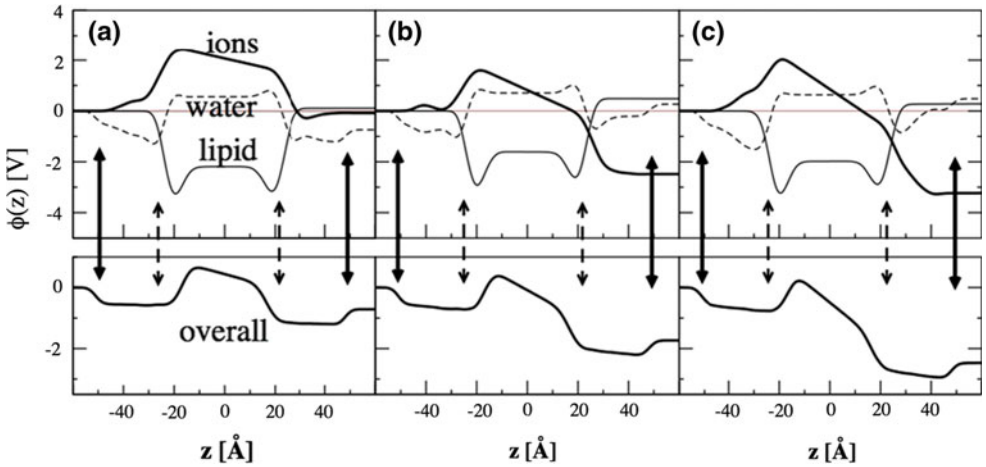


**Fig. 5** Components of the electrostatic potential profiles, $\phi(z)$, along the lipid bilayer normal, $z$, of a POPC membrane estimated from the initial stage of MD simulations of the system at 1 M NaCl salt concentration using the single bilayer method. $z = 0$ represents here the center of the lipid bilayer, *broken arrow* indicates the location of the bilayer–water interfaces and *solid arrows* show the locations of the air–water interfaces. From **a** to **c** increasing amounts of net charge imbalance $Q$ between the lower and upper electrolytes induce TM voltages (that may be estimated from the difference between the electrostatic potentials of the two water baths) of increasing amplitudes. Shown in the *top panels* are the contributions from lipid, water and ions and in the *lower panels* the total electrostatic potential. Note that the most of the TM voltage is due to the contribution from ions

200 mM NaCl salt solution. The system contains over 1,400 lipid molecules, forming a liposome of internal diameter of 8 nm. The system size ($210 \times 210 \times 210$ Å$^3$) was chosen to be large enough to avoid interaction between the central liposome and its replica, resulting in an overall number of $\sim$890,000 atoms. In such a setup a charge imbalance, $Q$, was imposed after the system equilibration between the inner and outer sides of the liposome.

Figure 5 reports the electrostatic potential profiles along the normal to the membrane generated from MD simulations of a POPC bilayer in contact with 1 M NaCl saltwater baths set at three increasing charge imbalances, $Q$, using the single bilayer method. Here, the electrostatic profiles are computed by considering also the charges of ions present in the system. For all simulations, the profiles computed at the initial stage show plateau values in the aqueous regions and, for increasing $Q$, an increasing potential difference $\Delta V$ between the two electrolytes indicative of a TM potential.

Quite interestingly, the profiles show clearly that, in contrast to the electric field case where the TM voltage is mainly due to the water dipole reorientation (Fig. 2), most of the voltage drop in the charge imbalance method is due to a contribution from the ions. Indeed, the sole collapse of the electrostatic potential due to the charge imbalance separation by the membrane lipid core accounts for the largest part of $\Delta V$.

Using the charge imbalance setup, it was possible for the first time to directly demonstrate in silico that the simulated lipid bilayer behaves as a capacitor (Delemotte et al. 2008) (Fig. 6). Simulations at various charge imbalances, $Q$, show a linear variation of $\Delta V$ from which the capacitance can be estimated as $C = Q_s.\Delta V^{-1}$, where $Q_s$ is the charge imbalance per unit area. The capacitance values extracted from simulations are expected to depend on the lipid composition (charged or not) and on the force-field parameters used and as such constitutes a supplementary way of checking the accuracy of lipid force-field parameters used in the simulation. Here, in the case of POPC bilayers embedded in a 1 M solution of NaCl (Delemotte et al. 2008), the capacitance, $C$, amounts to 0.85 μF cm$^{-2}$, which is in reasonable agreement with the value usually assumed in the literature, e.g., 1.0 μF cm$^{-2}$ (Roux 1997; Sachs et al. 2004) and with recent measurements for planar POPC lipid bilayers in a 100 mM KCl solution (0.5 μF cm$^{-2}$).

For large enough induced TM voltages, the three protocols lead to electroporation of the lipid bilayer. As in the case of the electric field method, for $\Delta V$ above 1.5–2.5 volts, the electroporation process starts with the formation of water fingers that protrude inside the hydrophobic core of the membrane. Within nanoseconds, water wires bridging the two sides of the membrane under voltage stress appear. If the simulations are further expended, lipid headgroups migrate along one wire and form a hydrophilic connected pathway (Fig. 7).

Because salt solutions are explicitly considered in these simulations, ion conduction through the hydrophilic pores occurred following electroporation of the lipid bilayers. Details about the ionic transport through the pores formed within the bilayer core upon electroporation could be gathered (Gurtovenko et al. 2010). The MD simulations of the double bilayer system (Gurtovenko and Vattulainen

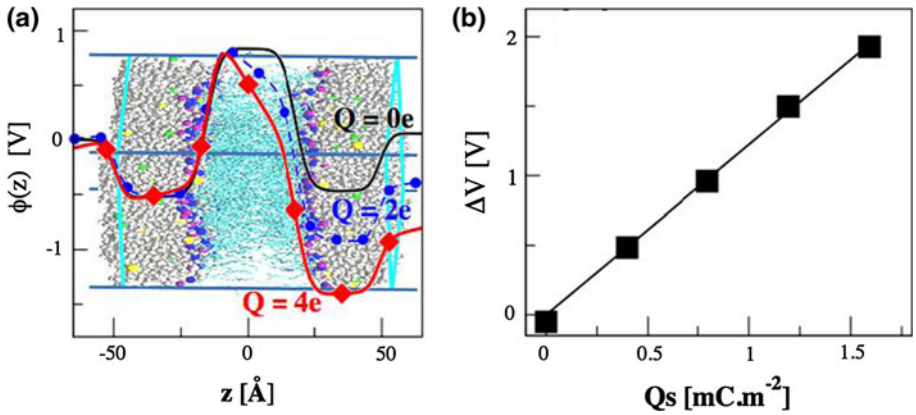


**Fig. 6** **a** Electrostatic potential, $\phi(z)$, across a POPC lipid bilayer for different net charge imbalances, $Q$, between the upper and lower electrolytes from MD simulations considering the setup of Fig. 5. $\phi(z)$ is estimated as an in-plane average of the EP distributions (Eq. 1). As a reference it was set to zero in the lower electrolyte. **b** TM potential, $\Delta V$, as a function of the charge imbalance, $Q_s$, per unit area. The capacitance ($C$) of the bilayer can be derived from the slope of the curve

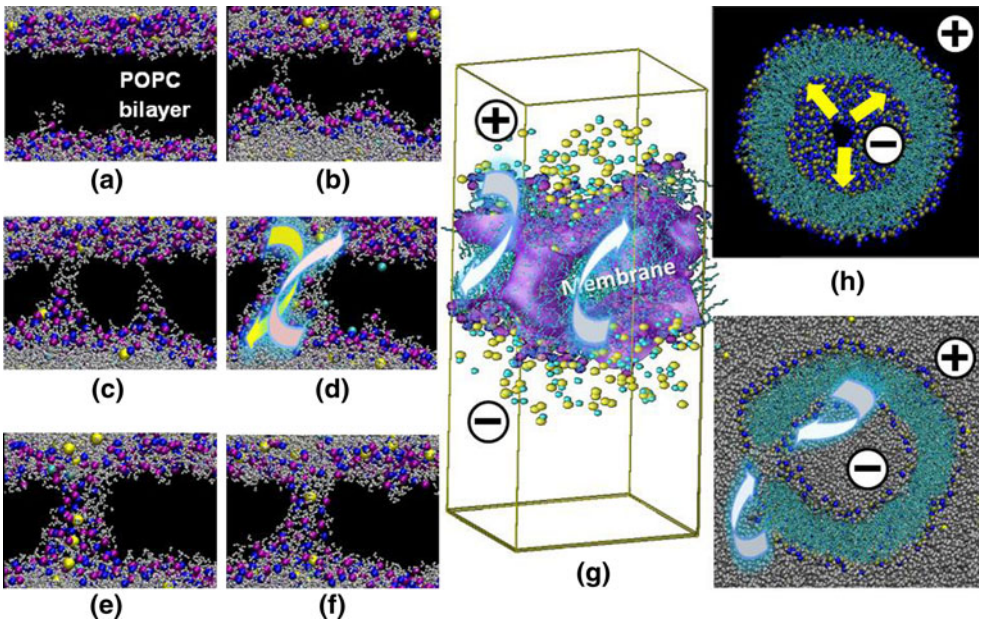


**Fig. 7** Sequence of events following the application of a TM voltage to a POPC lipid bilayer using the charge imbalance method (**a–f**). Note the migration of $Na^+$ (*yellow*) and $Cl^-$ (*cyan*) ions through the formed hydrophilic pores that are lined with lipid phosphate (*magenta*) and nitrogen (*blue*) headgroup atoms. **f** The state of a nonconducting pore reached when the exchange of ions between the two baths lowered $Q$ and therefore $\Delta V$ to values $\approx 200$ mV is shown. Topology of the nanometer-wide hydrophilic pores formed under high $\Delta V$ imposed by the charge imbalance method in the planar bilayer (**g**) and in the liposome (**h**). *Blue arrows* highlight the subsequent ionic flow through the pores, and the *yellow one* indicates the expansion of the pore as $\Delta V$ is maintained (Color figure online)

2005; Kandasamy and Larson 2006), and the results presented here for the single bilayer setup and for the liposome (Fig. 7) show that both cations and anions exchange through the pores between the two baths, with an overall flux of charges directed toward a decrease of the charge imbalance. Ion translocation through the pores from one bulk region to the other lasts from a few tens to a few hundreds of picoseconds and leads to a decrease of the charge imbalance and, hence, to the collapse of $\Delta V$. Hence, for all systems, when the charge imbalance reached a level where the TM voltage was down to a couple of hundred millivolts, the pores "closed" or "collapsed" in the sense that no more ionic translocation occurred (Fig. 7f). The final topology of the pores toward the end of the simulations remained stable for time spans exceeding the 10-ns scale, showing as reported in previous simulations (Tarek 2005) that complete recovery of the original bilayer structure requires a much longer time scale.

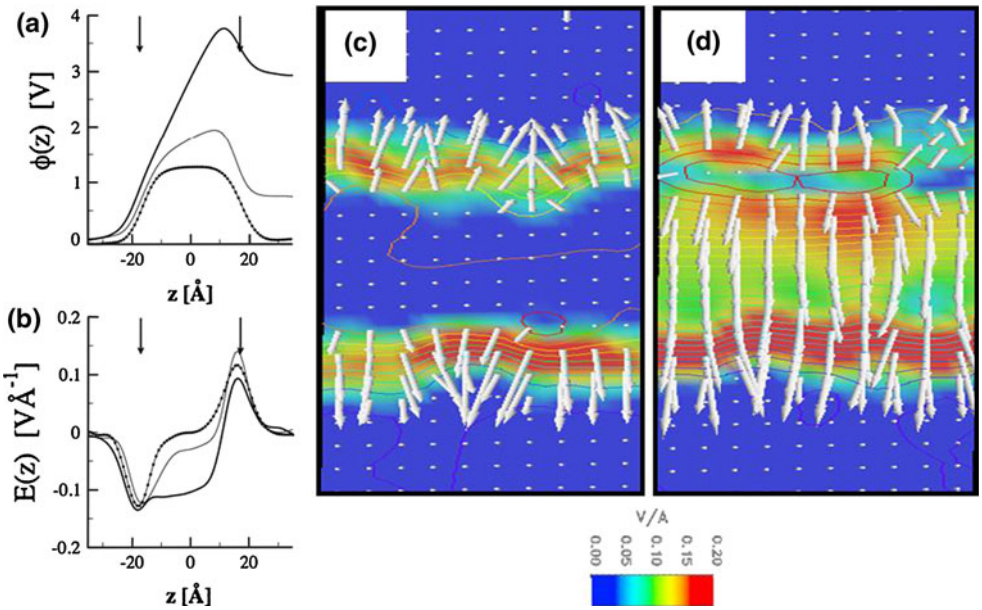


**Fig. 8** **a** Electrostatic potential profiles, $\phi(z)$, across a lipid bilayer subject to electric fields of 0.0 $V\text{Å}^{-1}$ (*dotted line*), 0.6 $V\text{Å}^{-1}$ (*thin line*) and 3.0 $V\text{Å}^{-1}$ (*bold line*). *Black arrows* point to the location of the lipid headgroups–water interface. **b** Corresponding electric field profiles derived as $\partial\phi(z)/\partial z$. **c** Two-dimensional (*out of plane*) map of the electric field distribution at 0.0 $V\text{Å}^{-1}$. The local electric field direction and strength are displayed as *white arrows*. Note that the larger fields are located at the lipid–water interfaces and oriented toward the solvent. **d** Two-dimensional (out of plane) map of the electric field distribution at 3.0 $V\text{Å}^{-1}$. *Note* the large fields located in the lipid core

Note that in order to maintain $\Delta V$ constant the modeler needs to maintain the initial charge imbalance by "injecting" charges (ions) in the electrolytes at a pace equivalent to the rate of ion translocation through the hydrophilic pore. This protocol is, particularly for the single bilayer setup, adequate for performing simulations under constant voltage (low voltage, millisecond duration) or constant current conditions, which is suitable for comparison to experiments undertaken under similar conditions (Kutzner et al. 2011).

## Discussion

MD simulations of lipid bilayers subject to high enough TM voltages, regardless of how the latter are generated, i.e., either by a direct electric field effect or by charging of the membranes, undergo a similar cascade of events: within a very short (nanosecond) time scale a defect in the membrane manifested by the protrusion of water fingers from the lipid headgroups/solvent forms in the lipid core. When the TM voltage is maintained, these fingers span the entire hydrophobic core, forming hydrophilic pores that are later stabilized by lipid headgroups. The time scales associated with each of these processes appear to be similar in both protocols. Finally, when the pulses are switched off, the pores collapse (close) within the same time scales. Accordingly, the MD simulations show clearly that, at the membrane level, the effects of nanosecond, megavolt-per-meter pulsed electric fields and of low-voltage, millisecond pulses are very similar. In the following we further investigate the molecular reasons leading to such similarities.

In order to determine the detailed mechanism of the pore creation, it is helpful to probe the electric field distribution across the bilayer, both at rest and under the effect of a TM voltage. Figure 8a displays the electrostatic potential profiles for a lipid bilayer subject to increasing electric fields that generate TM potentials ranging from 0 to $\sim$3 V. At 0 V, the lipid bilayer is at rest and the profiles reveal, in agreement with experiments (Liberman and Topaly 1969), the existence of a positive potential difference between the membrane interior and the adjacent aqueous phases.

At rest, the voltage change across the lipid–water interfaces, the so-called dipole potential (Fig. 1), gives rise locally to large electric fields. The latter, estimated simply as $\partial\phi(z)/\partial z$ (in the present case up to 1.5 V $\text{nm}^{-1}$), is oriented toward the bulk, while at the center of the bilayer the local electric field is null (Fig. 8b, c). When external electric fields of magnitudes, respectively, of 0.06 and 0.30 V $\text{nm}^{-1}$ are applied, reorientation of the water molecules gives rise to TM potentials of $\sim$0.75 and 3 V. Figure 8b, c reveals the incidence of such reorganization on the local electric field both at the interfacial region and within the bilayer core. In particular one notes that the field in the membrane core has

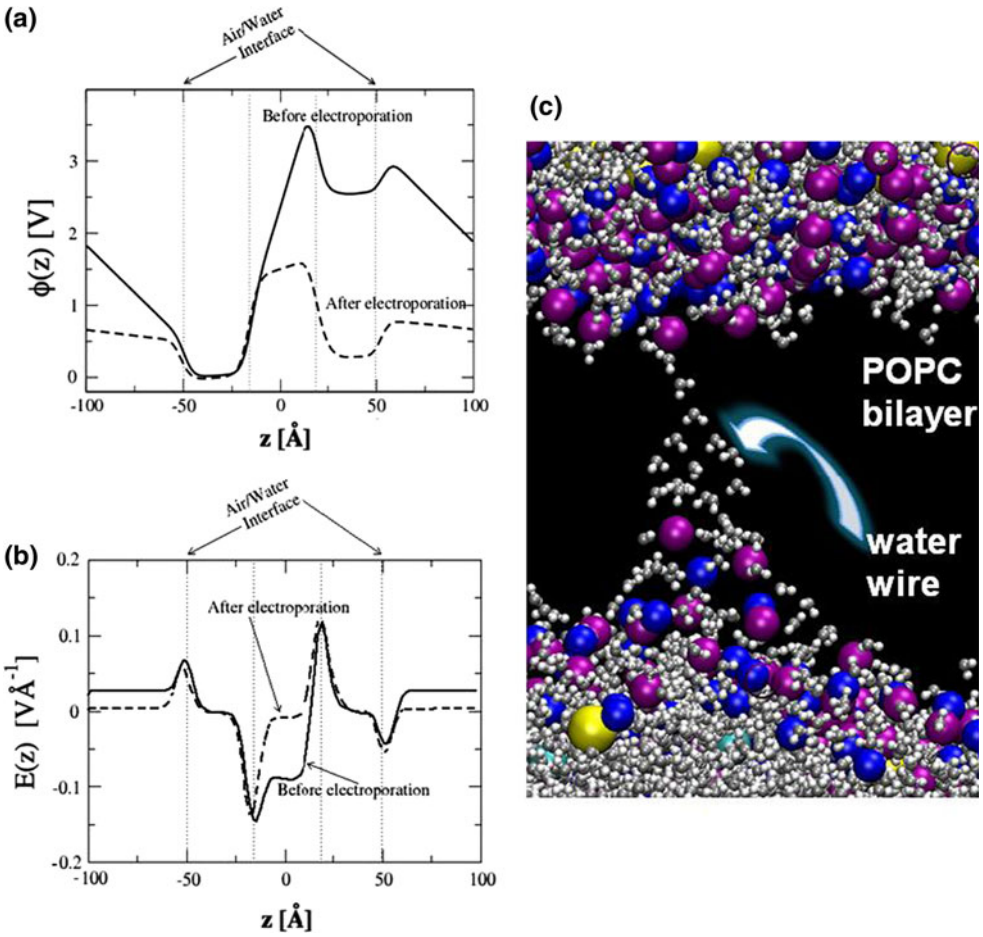


**Fig. 9** **a** Electrostatic potential profiles, $\phi(z)$, across a POPC lipid membrane subject to a charge imbalance (single bilayer setup) before (*solid line*) and after (*broken line*) electroporation. **b** Corresponding electric field profiles. **c** Snapshot taken from the MD simulation of the lipid bilayer subject to a TM voltage taken at the early stage of the pore formation showing the configuration of water molecules represented as balls and sticks (oxygen, *gray*) and (hydrogen, *white*) forming a continuous wire through the hydrophobic core of the membrane

risen to a value of $\sim 1$ V nm$^{-1}$ for the highest $\Delta V$ imposed. For the charge imbalance method, the overall picture is similar (Fig. 9a, b), where again the TM voltages created give rise to large electric fields within the membrane core, oriented perpendicular to the bilayer.

Qualitatively, the electric field method and the charge imbalance method result in a similar cascade of events that take place at the membrane, which is a direct consequence of such a field distribution. Indeed, water molecules, initially restrained to the interfacial region as they randomly percolate down within the membrane core, are subject to a high electric field and therefore inclined to orient their dipole along this local field. These molecules can easily hydrogen-bond among themselves, which results in the creation of water files. Such fingers protrude through the hydrophobic core from both sides of the membrane. Finally, these fingers meet up to form water channels (often termed "prepores" or "hydrophobic pores") that span the membrane (Fig. 9c). As the TM voltage is maintained, these water wires appear to be able to overcome the free energy barrier associated with the formation of a water molecule file that spans the bilayer (estimated to be $\sim 108$ kJ/mol in the absence of external electric field (Marrink et al. 1996). As the electrical stress is maintained, lipid headgroups migrate along the stable water wires and participate in the formation of larger "hydrophilic pores," able to conduct ions and larger molecules as they expand. Evidently, reorientation of the lipids depends not only on the net charges their headgroup carries, as has been shown for negatively charged phosphatidylserines that can move from one leaflet of the bilayer to the other, but also on the nature of the tails (Vernier et al. 2009).

## Conclusion

Currently, computational approaches remain potentially the only techniques able to follow, at the atomic scale, the local perturbation lipid membranes undergo when they are subjected to external electric field. The results obtained so far are believed to capture the essence of several aspects of the electroporation phenomena in bilayer membranes and could serve as an additional, complementary source of information to the current arsenal of experimental tools. At rest, i.e., before membrane breakdown, many characteristics of the bilayer (e.g., hydrophobic core thickness, area

per lipid, intrinsic dipole potential, capacitance) are in satisfactory agreement with experiments which indicate that the force fields and protocols used in MD simulations of lipid bilayers are rather well optimized. Despite their intrinsic differences, all MD simulations of lipid bilayers subjected to high enough TM voltages, regardless of how the latter are generated, provide support to the stochastic pore-formation theories in which the stress imposed on the membrane is released thanks to formation of nanometer-scale hydrophilic pores that span the lipid core. Quite interestingly, it was shown that pore time formation is similar for the electric field method and the charge imbalance method (Vernier et al. 2006b). Hence, MD simulations show clearly that at the membrane level the effects of nanosecond, megavolt-per-meter pulsed electric fields and of low-voltage, millisecond pulses are very similar.

There are several points that need further investigation. Perhaps the most important one is the interplay between pore densities (number of hydrophilic pores per unit area that can form) and transport rate that can be maintained at a given imposed voltage or current condition. Simulations have shown (Tarek 2005), as predicted (Lewis 2003), that upon pore creation the electric field induces a significant lateral stress, of the order of 1 mN $m^{-1}$. It is unclear how the induced lateral tension relaxes in a macroscopic system when a voltage pulse is applied, which may have an incidence on the density of pores that could nucleate. Regardless of the topology of the bilayer, i.e., in planar lipid membranes or in a liposome, one expects a strong correlation between the size of the defect created, the density of pores and the maintained electrical stress. Simulations of very large systems or those of liposomes should in principle help us to characterize better such a correlation.

It is undeniable that much more effort is still needed in order to determine the cascade of events involved in more complex events such as the transport of large molecules across the membranes.

**Acknowledgments** The research was conducted in the scope of the EBAM European Associated Laboratory (LEA). Simulations were performed using HPC resources from GENCI-CINES (grant 2010-2011 075137). M. T. acknowledges the support of the French Agence Nationale de la Recherche (grant ANR-10_BLAN-916-03-INTCELL).

## References

Abidor IG, Arakelyan VB, Chernomordink LV, Chizmadzhev YA, Pastushenko VF, Tarasevich MR (1979) Electrical breakdown of BLM: main experimental facts and their qualitative discussion. Bioelectrochem Bioenerg 6:37–52

Aksimentiev A, Schulten K (2005) Imaging α-hemolysin with molecular dynamics: ionic conductance, osmotic permeability, and the electrostatic potential map. Biophys J 88:3745–3761

Allen MP, Tildesley DJ (1987) Computer simulation of liquids. Clarendon Press, Oxford

Anézo C, Vries AHd, Höltje HD, Tieleman DP, Marrink SJ (2003) Methodological issues in lipid bilayer simulations. J Phys Chem B 107:9424–9433

Beebe SJ, Schoenbach KH (2005) Nanosecond pulsed electric fields: a new stimulus to activate intracellular signaling. J Biomed Biotechnol 4:297–300

Benz R, Beckers F, Zimmerman U (1979) Reversible electrical breakdown of lipid bilayer membranes—a charge-pulse relaxation study. J Membr Biol 48:181–204

Berkowitz ML, Raghavan MJ (1991) Computer simulation of a water/membrane interface. Langmuir 7:1042–1044

Berkowitz ML, Bostick DL, Pandit S (2006) Aqueous solutions next to phospholipid membrane surfaces: insights from simulations. Chem Rev 106(4):1527–1539

Bhandarkar M, Brunner R, Chipot C, Dalke A, Dixit S, Grayson P, Gullinsrud J, Gursoy A, Humphrey W, Hurwitz D, Krawetz N, Nelson M, Phillips J, Shinozaki A, Zheng G, Zhu F (2002) NAMD version 2.4. http://wwwksuiucedu/Research/namd

Bockmann RA, de Groot BL, Kakorin S, Neumann E, Grubmuller H (2008) Kinetics, statistics, and energetics of lipid membrane electroporation studied by molecular dynamics simulations. Biophys J 95:1837–1850

Bostick D, Berkowitz ML (2003) The implementation of slab geometry for membrane-channel molecular dynamics simulations. Biophys J 85:97–107

Cascales JJL, Berendsen HJC, de la Torre JG (1996) Molecular dynamics simulation of water between two charged layers of dipalmitoylphosphatidylserine. J Phys Chem 100:8621–8627

Chang DC (1992) Structure and dynamics of electric field-induced membrane pores as revealed by rapid-freezing electron microscopy. In: Guide to electroporation and electrofusion. Academic Press, Orlando, pp 9–27

Chen C, Smye SW, Robinson MP, Evans JA (2006) Membrane electroporation theories: a review. Med Biol Eng Comput 44:5–14

Chimerel C, Movileanu L, Pezeshki S, Winterhalter M, Kleinekathofer U (2008) Transport at the nanoscale: temperature dependence of ion conductance. Eur Biophys J 38:121–125

Chipot C, Klein ML, Tarek M (2005) Modeling lipid membranes. In: Yip S (ed) Handbook of materials modeling. Springer, Dordrecht, pp 929–958

Chiu SW, Clark M, Jakobsson E, Subramaniam S, Scott HL (1999) Optimization of hydrocarbon chain interaction parameters: application to the simulation of fluid phase lipid bilayers. J Phys Chem B 103:6323–6327

Chiu SW, Vasudevan S, Jakobsson E, Mashl RJ, Scott HL (2003) Structure of sphingomyelin bilayers: a simulation study. Biophys J 85:3624–3635

Crozier PS, Henderson D, Rowley RL, Busath DD (2001) Model channel ion currents in NaCl extended simple point charge water solution with applied-field molecular dynamics. Biophys J 81:3077–3089

Dahlberg M, Maliniak A (2008) Molecular dynamics simulations of cardiolipin bilayers. J Phys Chem B 112:11655–11663

Damodaran KV, Merz KM (1994) A comparison of DMPC and DLPE-based lipid bilayers. Biophys J 66:1076–1087

Darden T, York D, Pedersen L (1993) Particle mesh ewald—an N log(N) method for Ewald sums in large systems. J Chem Phys 98:10089–10092

Delemotte L, Dehez F, Treptow W, Tarek M (2008) Modeling membranes under a transmembrane potential. J Phys Chem B 112:5547–5550

Delemotte L, Treptow W, Klein ML, Tarek M (2010) Effect of sensor domain mutations on the properties of voltage-gated ion channels: molecular dynamics studies of the potassium channel Kv1.2. Biophys J 99(9):L72–L74

Delemotte L, Tarek M, Klein ML, Amaral C, Treptow W (2011) Intermediate states of the Kv1.2 voltage sensor from atomistic molecular dynamics simulations. Proc Natl Acad Sci USA 108(15):6109–6114

Deng J, Schoenbach KH, Buescher ES, Hair PS, Fox PM, Beebe SJ (2003) The effects of intense submicrosecond electrical pulses on cells. Biophys J 84:2709–2714

Eberhard N, Sowers AE, Jordan CA (1989) Electroporation and electrofusion in cell biology. Plenum Press, New York

Edholm O (2008) Time and length scales in lipid bilayer simulations. In: Feller SE (ed) Computational modeling of membrane bilayers, vol 60. Current topics in membranes. Elsevier, London, pp 91–110

Essmann U, Perera L, Berkowitz ML, Darden T, Pedersen LG (1995) A smooth particle mesh Ewald method. J Chem Phys 103: 8577–8593

Feller SE (2000) Molecular dynamics simulations of lipid bilayers. Curr Opin Colloid Interface Sci 5:217–223

Feller SE (2008) Computational modeling of membrane bilayers, vol 60. current topics in membranes. Elsevier, London

Feller SE, Gawrisch K, MacKerell AD (2002) Polyunsaturated fatty acids in lipid bilayers: intrinsic and environmental contributions to their unique physical properties. J Am Chem Soc 124:318–326

Forrest LR, Sansom MSP (2000) Membrane simulations: bigger and better. Curr Opin Struct Biol 10:174–181

Gawrisch K, Ruston D, Zimmerberg J, Parsegian V, Rand R, Fuller N (1992) Membrane dipole potentials, hydration forces, and the ordering of water at membrane surfaces. Biophys J 61:1213–1223

Gennis RB (1989) Biomembranes: molecular structure and function. Springer, Heidelberg

Gillilan RE, Wood F (1995) Visualization, virtual reality, and animation within the data flow model of computing. Comput Graph 29:55–58

Golzio M, Teissie J, Rols M-P (2002) Direct visualization at the single-cell level of electrically mediated gene delivery. Proc Natl Acad Sci USA 99:1292–1297

Gurtovenko AA, Vattulainen I (2005) Pore formation coupled to ion transport through lipid membranes as induced by transmembrane ionic charge imbalance: atomistic molecular dynamics study. J Am Chem Soc 127:17570–17571

Gurtovenko AA, Vattulainen I (2008) Effect of NaCl and KCl on phosphatidylcholine and phosphatidylethanolamine lipid membranes: insight from atomic-scale simulations for understanding salt-induced effects in the plasma membrane. J Phys Chem B 112:1953–1962

Gurtovenko AA, Jamshed Anwar J, Vattulainen I (2010) Defect-mediated trafficking across cell membranes: insights from in silico modeling. Chem Rev 110:6077–6103

Hu Q, Viswanadham S, Joshi RP, Schoenbach KH, Beebe SJ, Blackmore PF (2005) Simulations of transient membrane behavior in cells subjected to a high-intensity ultrashort electric pulse. Phys Rev E 71:031914

Humphrey W, Dalke A, Schulten K (1996) VMD—visual molecular dynamics. J Mol Graph 14:33–38

Kalé L, Skeel R, Bhandarkar M, Brunner R, Gursoy A, Krawetz N, Phillips J, Shinozaki A, Varadarajan K, Schulten K (1999) Namd2: greater scalability for parallel molecular dynamics. J Comp Phys 151:283–312

Kandasamy SK, Larson RG (2006) Cation and anion transport through hydrophilic pores in lipid bilayers. J Chem Phys 125:074901

Khalili-Araghi F, Tajkhorshid E, Schulten K (2006) Dynamics of $K^+$ ion conduction through Kv1.2. Biophys J 91:L72–L74

Kotnik T, Miklavcic D (2006) Theoretical evaluation of voltage inducement on internal membranes of biological cells exposed to electric fields. Biophys J 90(2):480–491

Kotnik T, Miklavcic D, Slivnik T (1998) Time course of transmembrane voltage induced by time-varying electric fields—a method for theoretical analysis and its application. Bioelectrochem Bioenerg 45(1):3–16

Kutzner C, Grubmüller H, de Groot BL, Zachariae U (2011) Computational electrophysiology: the molecular dynamics of ion channel permeation and selectivity in atomistic detail. Biophys J 101:809–817

Leach AR (2001) Molecular modelling: principles and applications, 2nd edn. Prentice Hall, Englewood Cliffs

Lewis TJ (2003) A model for bilayer membrane electroporation based on resultant electromechanical stress. IEEE Trans Dielectr Electr Insul 10:769–777

Li S (2008) Electroporation protocols: preclinical and clinical gene medicine, vol 423. Methods in molecular biology. Humana Press, Totowa

Li Z, Venable RM, Rogers LA, Murray D, Pastor RW (2009) Molecular dynamics simulations of PIP2 and PIP3 in lipid bilayers: determination of ring orientation, and the effects of surface roughness on a Poisson-Boltzmann description. Biophys J 97:155–163

Liberman YA, Topaly VP (1969) Permeability of biomolecular phospholipid membranes for fat-soluble ions. Biophysics USSR 14:477

Lindahl E, Edholm O (2000) Mesoscopic undulations and thickness fluctuations in lipid bilayers from molecular dynamics simulations. Biophys J 79:426–433

Lindahl E, Sansom MSP (2008) Membrane proteins: molecular dynamics simulations. Curr Opin Struct Biol 18:425–431

MacKerell AD Jr, Bashford D, Bellott M, Dunbrack RL Jr, Evanseck J, Field MJ, Fischer S, Gao J, Guo H, Ha S, Joseph-McCarthy D, Kuchnir L, Kuczera K, Lau FTK, Mattos C, Michnick S, Ngo T, Nguyen DT, Prodhom B, Reiher WE III, Roux B, Schlenkrich M, Smith JC, Stote R, Straub J, Watanabe M, Wiorkiewicz-Kuczera J, Yin D, Karplus M (1998) All-atom empirical potential for molecular modeling and dynamics studies of proteins. J Phys Chem B 102:3586–3616

Marrink SJ, Mark AE (2001) Effect of undulations on surface tension in simulated bilayers. J Phys Chem B 105:6122–6127

Marrink SJ, Jähniga F, Berendsen HJ (1996) Proton transport across transient single-file water pores in a lipid membrane studied by molecular dynamics simulations. Biophys J 71:632–647

Marrink SJ, de Vries AH, Tieleman DP (2009) Lipids on the move: simulations of membrane pores, domains, stalks and curves. Biochim Biophys Acta Biomembr 1788:149–168

Mashl RJ, Scott HL, Subramaniam S, Jakobsson E (2001) Molecular simulation of dioleylphosphatidylcholine bilayers at differing levels of hydration. Biophys J 81:3005–3015

Mukhopadhyay P, Monticelli L, Tieleman DP (2004) Molecular dynamics simulation of a palmitoyl-oleoyl phosphatidylserine bilayer with $Na^+$ counterions and NaCl. Biophys J 86:1601–1609

Nickoloff JA (1995) Animal cell electroporation and electrofusion protocols, vol 48. Methods in molecular biology. Humana Press, Totowa

Paganin-Gioannia A, Bellarda E, Escoffrea JM, Rols MP, Teissié J, Golzio M (2011) Direct visualization at the single-cell level of siRNA electrotransfer into cancer cells. Proc Natl Acad Sci USA 108:10443–10447

Pandit SA, Bostick D, Berkowitz ML (2003) Mixed bilayer containing dipalmitoylphosphatidylcholine and dipalmitoylphosphatidylserine: lipid complexation, ion binding, and electrostatics. Biophys J 85:3120–3131

Patel RY, Balaji PV (2008) Characterization of symmetric and asymmetric lipid bilayers composed of varying concentrations of ganglioside $GM_1$ and DPPC. J Phys Chem B 112:3346–3356

Pauly H, Schwan HP (1959) Uber die Impedanz Einer Suspension von Kugelformigen Teilchen mit Einer Schale—Ein Modell fur das Dielektrische Verhalten von Zellsuspensionen und von Proteinlosungen. Z Naturforsch B 14(2):125–131

Pucihar G, Kotnik T, Valic B, Miklavcic D (2006) Numerical determination of transmembrane voltage induced on irregularly shaped cells. Ann Biomed Eng 34:642–652

Pucihar G, Kotnik T, Miklavcic D, Teissié J (2008) Kinetics of transmembrane transport of small molecules into electropermeabilized cells. Biophys J 95:2837–2848

Rog T, Martinez-Seara H, Munck N, Oresic M, Karttunen M, Vattulainen I (2009) Role of cardiolipins in the inner mitochondrial membrane: insight gained through atom-scale simulations. J Phys Chem B 113:3413–3422

Rög T, Murzyn K, Pasenkiewicz-Gierula M (2002) The dynamics of water at the phospholipid bilayer: a molecular dynamics study. Chem Phys Lett 352:323–327

Roux B (1997) Influence of the membrane potential on the free energy of an intrinsic protein. Biophys J 73:2980–2989

Roux B (2008) The membrane potential and its representation by a constant electric field in computer simulations. Biophys J 95:4205–4216

Sachs JN, Crozier PS, Woolf TB (2004) Atomistic simulations of biologically realistic transmembrane potential gradients. J Chem Phys 121:10847–10851

Saiz L, Klein ML (2001) Structural properties of a highly polyunsaturated lipid bilayer from molecular dynamics simulations. Biophys J 81:204–216

Saiz L, Klein ML (2002a) Computer simulation studies of model biological membranes. Acc Chem Res 35:482–489

Saiz L, Klein ML (2002b) Electrostatic interactions in a neutral model phospholipid bilayer by molecular dynamics simulations. J Chem Phys 116:3052–3057

Sotomayor M, Vasquez V, Perozo E, Schulten K (2007) Ion conduction through MscS as determined by electrophysiology and simulation. Biophys J 92:886–902

Sundararajan R (2009) Nanosecond electroporation: another look. Mol Biotechnol 41:69–82

Tarek M (2005) Membrane electroporation: a molecular dynamics simulation. Biophys J 88:4045–4053

Tieleman DP (2004) The molecular basis of electroporation. BMC Biochem 5:10

Tieleman DP, Marrink SJ, Berendsen HJC (1997) A computer perspective of membranes: molecular dynamics studies of lipid bilayer systems. Biochim Biophys Acta 1331:235–270

Tieleman DP, Berendsen JHC, Sansom MSP (2001) Voltage-dependent insertion of alamethicin at phospholipid/water and octane water interfaces. Biophys J 80:331–346

Tobias DJ (2001) Membrane simulations. In: Becker OH, Roux B, Watanabe M (eds) Computational biochemistry and biophysics. Marcel Dekker, New York

Tobias DJ, Tu K, Klein ML (1997) Atomic-scale molecular dynamics simulations of lipid membranes. Curr Opin Colloid Interface Sci 2:15–26

Treptow W, Maigret B, Chipot C, Tarek M (2004) Coupled motions between pore and voltage-sensor domains: a model for *Shaker* B, a voltage-gated potassium channel. Biophys J 87:2365–2379

Treptow W, Tarek M, Klein ML (2009) Initial response of the potassium channel voltage sensor to a transmembrane potential. J Am Chem Soc 131:2107–2110

Vacha R, Berkowitz ML, Jungwirth P (2009) Molecular model of a cell plasma membrane with an asymmetric multicomponent composition: water permeation and ion effects. Biophys J 96:4493–4501

Vasilkoski Z, Esser AT, Gowrishankar TR, Weaver JC (2006) Membrane electroporation: the absolute rate equation and nanosecond time scale pore creation. Phys Rev E 74:021904

Vernier PT, Ziegler MJ (2007) Nanosecond field alignment of head group and water dipoles in electroporating phospholipid bilayers. J Phys Chem B 111:12993–12996

Vernier PT, Ziegler MJ, Sun Y, Chang WV, Gundersen MA, Tieleman DP (2006a) Nanopore formation and phosphatidylserine externalization in a phospholipid bilayer at high transmembrane potential. J Am Chem Soc 128:6288–6289

Vernier PT, Ziegler MJ, Sun Y, Gundersen MA, Tieleman DP (2006b) Nanopore-facilitated, voltage-driven phosphatidylserine translocation in lipid bilayers—in cells and in silico. Phys Biol 3:233–247

Vernier PT, Levine ZA, Wu H-S, Joubert V, Ziegler MJ, Mir LM, Tieleman DP (2009) Electroporating fields target oxidatively damaged areas in the cell membrane. PLoS ONE 4:e7966

Weaver JC (2003) Electroporation of biological membranes from multicellular to nano scales. IEEE Trans Dielectr Electr Insul 10:754–768

Weaver JC, Chizmadzhev YA (1996) Theory of electroporation: a review. Bioelectrochem Bioenerg 41:135–160

Wiener MC, White SH (1992) Structure of fluid dioleylphosphatidylcholine bilayer determined by joint refinement of X-ray and neutron diffraction data. III. Complete structure. Biophys J 61:434–447

Yang Y, Henderson D, Crozier P, Rowley RL, Busath DD (2002) Permeation of ions through a model biological channel: effect of periodic boundary condition and cell size. Mol Phys 100: 3011–3019

Zhong Q, Moore PB, Newns DM, Klein ML (1998) Molecular dynamics study of the LS3 voltage-gated ion channel. FEBS Lett 427:267–270

Ziegler MJ, Vernier PT (2008) Interface water dynamics and porating electric fields for phospholipid bilayers. J Phys Chem B 112: 13588–13596